Intercalation of Nitroanilines into Kaolinite and Second Harmonic Generation

Ryoji Takenawa,[†] Yoshihiko Komori,[‡] Shigenobu Hayashi,[‡] Jun Kawamata,[§] and Kazuyuki Kuroda*[,†,||]

Department of Applied Chemistry, Waseda University, Ohkubo-3, Shinjuku-ku, Tokyo 169-8555, Japan, National Institute of Materials and Chemical Research, Higashi 1-1, Tsukuba, Ibaraki, 305-8565, Japan, Research Institute for Electronic Science, Hokkaido University, Sapporo 060-0812, Japan, and Kagami Memorial Laboratory for Materials Science and Technology, Waseda University, Nishiwaseda-2, Shinjuku-ku, Tokyo 169-0051, Japan

Received February 2, 2001. Revised Manuscript Received April 13, 2001

Kaolinite intercalates *ortho*- and *para*-nitroanilines (*o*NA and *p*NA) between the layers whereas *meta*-nitroaniline (*m*NA) is not intercalated. *para*-Nitroaniline takes a monolayer arrangement with the long axis inclined to the layers of kaolinite. *o*NA molecules also take a monolayer arrangement though the orientation is not well ordered. Kaolinite−*p*NA and −*o*NA intercalation compounds exhibit second harmonic generation, which is evaluated quantitatively by the second-harmonic wave generated with evanescent wave (SHEW) method. This indicates noncentrosymmetric arrangements of *p*NA and *o*NA, and such orientations are induced by the asymmetric environment of the interlayer region of kaolinite.

Introduction

Many inorganic layered materials can accommodate various types of organic species to form inorganic−organic intercalation compounds in which guest organic species reside in a confined two-dimensional space. Interactions between inorganic hosts and organic guest species are crucial for the design of this type of nanocomposite.[1−3] Inorganic layered materials are suitable for immobilizing and organizing guest species in the interlayers and outer surfaces.

Kaolinite, a clay mineral, is an aluminosilicate whose structure is composed of interstratified $AlO_2(OH)_4$ octahedral sheets and SiO_4 tetrahedral sheets. The two-dimensional nanospaces between the layers are sandwiched by the oxide sheets and the octahedral hydroxide layers. Consequently, the interlayer space is asymmetrical, which is not found in other layered materials. Only small polar molecules such as dimethyl sulfoxide (DMSO) and *N*-methylformamide (NMF) can be intercalated directly.[4] Those polar molecules take definite arrangements in the very confined region.[5] Consequently, kaolinite is useful for organizing guest species in a controlled manner.

Nonlinear optics has been investigated in various material systems. Organic molecules with very high second hyperpolarizabilities (β) have generally large dipole moments, but their assemblies or crystals normally have a center of symmetry that destructs second harmonic generation (SHG). Therefore, inclusion compounds such as cyclodextrin[6,7] and porous materials such as ZSM-5,[8] ALPO-5,[9] and MCM-41[10] have been employed to suppress the crystallization of organic species. Tetramethylammonium-exchanged saponite[11] and MPS_3[12] have also been used for unique arrangements of SHG active organic molecules by using outer electric charge and utilization of organic assemblies, respectively, to cause noncentrosymmetries by the use of host−guest interactions.

We have recently reported preliminarily that well-modified kaolinite can accommodate *para*-nitroaniline (*p*NA) between the layers.[13] It is well-known that *p*NA crystals do not exhibit second-order nonlinear optical properties because the crystals take centrosymmetry. By incorporation of *p*NA between the layers of kaolinite, SHG was observed clearly by a simple transmission mode due to the unique structure.[13] In the present study, intercalation of *ortho*-, *meta*-, and *para*-nitroanilines into kaolinite was examined. Intercalation behavior of kaolinite toward these molecules was different from each other and the unique arrangements of intercalated guest species in the interlayer region were discussed. The second-order nonlinear optical

[†] Department of Applied Chemistry, Waseda University.
[‡] National Institute of Materials and Chemical Research.
[§] Hokkaido University.
[||] Kagami Memorial Laboratory for Materials Science and Technology, Waseda University.

(1) Bruce, D. M.; O'Hare, D. *Inorganic Materials*, 2nd ed.; Wiley: New York, 1996.
(2) Ogawa, M.; Kuroda, K. *Chem. Rev.* **1995**, *95*, 399.
(3) Alberti, G.; Bein, T. *Comprehensive Supramolecular Chemistry*; Pergamon: Oxford, U.K., 1996; Vol. 7.
(4) Theng, B. K. G. *The Chemistry of Clay-Organic Reactions*; Adam Hilger: London, 1974; pp 1−260.
(5) Thompson, J. G.; Cuff, C. *Clays Clay Miner.* **1985**, *33*, 493.
(6) Tomaru, S.; Zenbutsu, S.; Kawachi, M.; Kobayashi, M. *J. Chem. Soc., Chem. Commun.* **1984**, 1207.
(7) Wang, Y.; Eaton, D. F. *Chem. Phys. Lett.* **1985**, *120*, 441.
(8) Caro, J.; Finger, G.; Kornatowski, J.; Richter-Mendau, J.; Werner, L.; Zibrowwius, B. *Adv. Mater.* **1992**, *4*, 273.
(9) Werner, L.; Caro, J.; Finger G.; Kornatowski, J. *Zeolites* **1992**, *12*, 658.
(10) Kinski, I.; Gies, H.; Marlow, F. *Zeolites* **1997**, *19*, 375.
(11) Ogawa, M.; Takahashi, M.; Kuroda, K. *Chem. Mater.* **1994**, *6*, 715.
(12) Lacroix, P. G.; Clément, R.; Nakatani, K.; Zyss, J.; Ladoux, I. *Science* **1994**, *263*, 658.
(13) Kuroda, K.; Hiraguri, K.; Komori, Y.; Sugahara, Y.; Mouri, H.; Uesu, Y. *Chem. Commun.* **1999**, 2253.

10.1021/cm010095j CCC: $20.00
Published on Web 07/11/2001

properties were also studied quantitatively by the second-harmonic wave generated with evanescent wave (SHEW) method that was developed in 1994 for the absolute determination of SHG properties of powders.[14] The advantage of the method is the capability of the estimation of effective *d* coefficients because the signal intensity depends on the largest tensor component regardless of the phase matching.[14]

Experimental Section

Materials. Kaolinite used in this study was KGa-1 (Georgia, Source Clays Repository of Clay Minerals Society, Boulder, CO) and was ground to pass a 100 mesh sieve. *para*-Nitroaniline (99.8%, Tokyo Kasei Co.) was recrystallized from ethanol. *ortho*-Nitroaniline (99%, Tokyo Kasei Co.) and *meta*-nitroaniline (Guaranteed Reagent grade, Kanto Chemical Co.) were used as received. Guaranteed reagent grade *N*-methylformamide (NMF) (Tokyo Kasei Co.) and methanol (Kanto Chemical Co.) were also used as received.

Synthesis of Intercalation Compounds. It is known that kaolinite can intercalate only small polar molecules,[4] and it has been reported that *para*-nitroaniline is not intercalated into kaolinite even by a displacement method.[15] Consequently, we used a kaolinite−methanol intercalation compound (kaolinite/methanol) as a highly versatile intermediate[16] for guest displacement reactions with nitroanilines. Kaolinite/methanol was prepared by stirring kaolinite/NMF in methanol.[16] Kaolinite/NMF was prepared by the reaction of kaolinite with an aqueous solution of NMF (90.9%).[17] The guest displacement reaction between NMF and methanol was repeated seven times for completion.

Wet kaolinite/methanol was added into an ethanol solution saturated with *o*NA, *m*NA, or *p*NA, and the mixture was stirred for 3 days at room temperature. After the reaction the product was centrifuged and the supernatant solution was removed. The XRD pattern of the reaction product of kaolinite with *o*NA showed the peaks due to *o*NA crystals. To remove *o*NA adsorbed onto the outer surface of kaolinite, the product was heated at 110 °C for 10 h. Intercalation of nitrobenzene and aniline was also performed for comparison to discuss the intercalation behavior of nitroanilines.

Analyses. Powder X-ray diffraction (XRD) patterns were obtained by a MAC Science MXP^3 diffractometer using graphite-monochromated Cu Kα radiation. Solid-state NMR spectra were recorded on a JEOL NM-GSX400. Resonance frequencies for ^{13}C and ^{29}Si were 100.4 and 79.3 MHz, respectively. The measurement mode was CP/MAS, and the samples were rotated at about 5 kHz. The contact time dependencies of the intensities of ^{29}Si CP/MAS NMR signals were determined with a Bruker ASX400 at a resonance frequency of 79.50 MHz and at a spinning rate of ca. 5 kHz. With regard to the ^{13}C NMR spectrum of kaolinite/*o*NA, a JEOL JMM-CMX400 spectrometer was employed. A resonance frequency for ^{13}C was 100.4 MHz. The measurement mode was CP/MAS, and the samples were rotated at about 11 kHz. CHN analysis was performed with a Perkin-Elmer 2400 II instrument. Thermogravimetry was conducted with a MAC Science TG-DTA 2000S with a heating rate of 10 °C/min under a dry air atmosphere. IR spectra were recorded by a Perkin-Elmer FTIR 1640 spectrometer by the KBr disk technique and by the Nujol technique. UV−vis spectra by a diffuse reflectance method were measured with a Shimadzu UV-3100PC spectrometer equipped with an integrating sphere by diluting samples (ca. 5%) with MgO powders.

Measurement of Second Harmonic Generation (SHG). The SHG intensities were evaluated quantitatively by the SHEW method[14] reported by Kiguchi et al. Effective second-order nonlinear optical coefficients d_{eff} are obtained by this method. Each sample was mounted into a sample holder by $2.0g \times 10^{-2}$ N m, where g is the gravitational acceleration, and irradiated by a 1 kHz Nd:YAG laser ($\lambda = 1064$ nm, 50 μJ/pulse). The d_{eff} coefficients were calculated by comparing the SHEW signal intensity of samples with that of a reference sample (urea) under the same conditions. It has already been reported that the intensity measured by this method does not depend on the particle size of samples.[14]

The SHG intensities of the samples with different *p*NA loadings were measured by a powder method of Kurtz et al.[18] Each sample was packed onto a slide glass by a thickness of 0.05 mm. The light source was a 10 Hz Nd:YAG laser (8.5−23.3 mJ/pulse); a light of $\lambda = 1064$ nm was irradiated on the samples, and the intensities of transmitted green light of $\lambda = 532$ nm were measured.

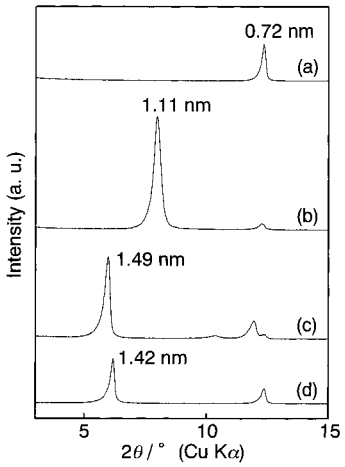

Figure 1. X-ray diffraction patterns of (a) kaolinite, (b) kaolinite−methanol intercalation compound, (c) kaolinite−*p*NA intercalation compound, and (d) kaolinite−*o*NA intercalation compound.

Results and Discussion

Figure 1 shows the XRD patterns of the reaction products. The basal spacing of kaolinite (0.72 nm) increased to 1.49 nm after the reaction with *p*NA and 1.42 nm with *o*NA. The spacing of the kaolinite−nitrobenzene intercalation compound was 1.45 nm. All these data are larger than that of kaolinite/methanol (1.11 nm), indicating intercalation of these molecules. On the other hand, the basal spacing of the product with *m*NA or aniline was 0.86 nm and the value is the same as that of dried kaolinite/methanol, suggesting that these molecules were not intercalated into kaolinite. Although alkylamines are intercalated into kaolinite by a displacement method,[19] the basicity of aniline is not so strong to interact with hydroxyl groups of kaolinite.

In the *o*NA and *p*NA systems, the resonance effect due to the π-electron system of the benzene ring occurs, and the nitro and amino groups exhibit large electron-withdrawing and electron-donating effects, respectively.[20] Accordingly, these molecules can have a large polarity and the nitro group can interact with the OH groups in kaolinite rather strongly. On the other hand, *m*NA has the donor and acceptor groups at the *meta* position, and therefore, the interactions with the OH

(14) Kiguchi, M.; Kato, M.; Kumegawa, N.; Taniguchi, Y. *J. Appl. Phys.* **1994,** *75*, 4332.
(15) Tunney, J.; Detellier, C. *Can. J. Chem.* **1997**, *75*, 1766.
(16) Komori, Y.; Sugahara, Y.; Kuroda, K. *J. Mater. Res.* **1998**, *13*, 930.
(17) Olejnik, S.; Posner, A. M.; Quirk, J. P. *Clay Miner.* **1970**, *8*, 421.
(18) Kurtz, S. K.; Perry, T. T. *J. Appl. Phys.* **1968**, *39*, 3798.
(19) Komori, Y.; Sugahara, Y.; Kuroda, K. *Appl. Clay Sci.* **1999**, *15*, 241.
(20) Levine, B. F. *Chem. Phys. Lett.* **1976**, *37*, 516.

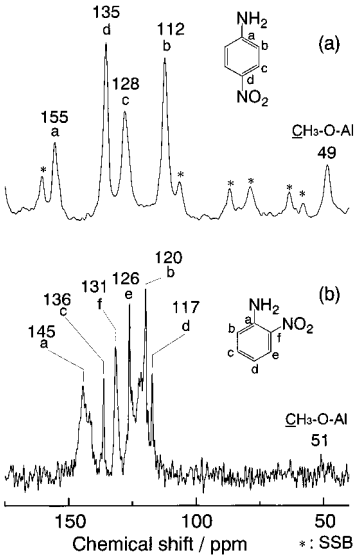

Figure 2. ^{13}C CP/MAS NMR spectrum of (a) kaolinite−*p*NA intercalation compound (MAS spinning rate 5 kHz) and (b) kaolinite−*o*NA intercalation compound (MAS spinning rate 11 kHz).

groups are less intense because of the lacking of the resonance effect.

Other organic species (*N*-methyl-*p*-nitroaniline, *N*,*N*-dimethyl-*p*-nitroaniline, 2-amino-5-nitropyrimidine, 2-amino-5-nitropyridine, 4-amino-4′-nitrobiphenyl, 4-amino-4′-nitroazobenzene (Disperse Orange 3), and 4-(dimethylamino)-4′-nitrostilbene (DANS)) were not intercalated into kaolinite. The reason for these findings probably comes from the relatively large molecular sizes of these species as well as their weak interactions with the interlayer surface of kaolinite.

Characterization of Kaolinite/*p*NA. The ^{13}C CP/MAS NMR spectrum of kaolinite/*p*NA is shown in Figure 2. The signals at 112, 128, 135, and 155 ppm are due to benzene ring of *p*NA. The signal at 49 ppm is ascribed to residual methoxy groups which are incorporated during the formation of kaolinite/methanol.[21] The content of *p*NA in kaolinite/*p*NA, calculated by CHN analysis, is 0.73 *p*NA per the structural unit of kaolinite [$Al_2Si_2O_5(OH)_4$]. Our previous communication reported that the amount was 0.6 *p*NA,[13] and the difference results from the difference in the solvents. Judging from these results, *p*NA molecules take a monolayer arrangement between the layers.

Probably, the main driving force for intercalation of *p*NA is the formation of hydrogen bonds between hydroxyl groups of kaolinite and electron-withdrawing nitro groups of *p*NA. This comes from the findings that nitrobenzene is intercalated into kaolinite but that aniline is not. Additionally, *N*,*N*-dimethyl-*p*-nitroaniline was not intercalated, suggesting that the amino groups of *p*NA also form hydrogen bonds with the silicate sheets. The kind of substituents of organic guest species is a major factor for intercalation of kaolinite, which will be very important for generalization of intercalation chemistry of kaolinite.

The variation of the Si environments caused by the interactions between the silicate sheets and *p*NA was

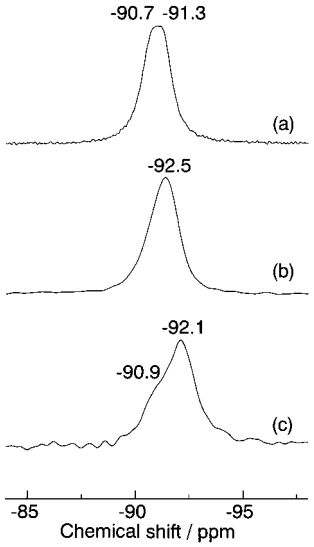

Figure 3. ^{29}Si CP/MAS NMR spectra of (a) kaolinite, (b) kaolinite−*p*NA intercalation conpound, and (c) kaolinite−*o*NA intercalation compound.

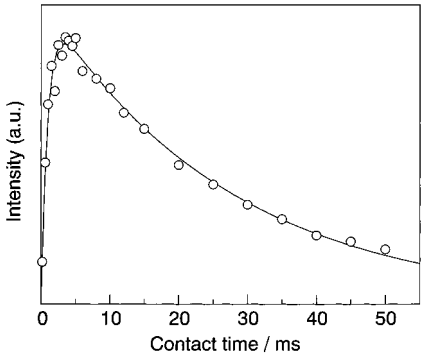

Figure 4. Contact time dependencies of the signal intensity in ^{29}Si CP/MAS NMR spectra of kaolinite−*p*NA intercalation compound (○). The solid line shows theoretical fitting as described in the text. The MAS spinning rate was 5 kHz.

investigated by ^{29}Si CP/MAS NMR (Figure 3). Kaolinite exhibits two resolved peaks due to Q^3 environments (Q^3: $OSi(OSi)_3$) at −90.7 and −91.3 ppm.[22,23] When kaolinite forms organic intercalation compounds, the splitting disappears and the chemical shifts depend on the guest species.[5] The single peak at −91.5 ppm was observed on the intercalation of *p*NA. Because similar shifts have been observed for kaolinite/alkylamines,[19] the result supports the interactions between amino groups and the silicate sheets.

The contact time dependencies of the ^{29}Si signals intensity derived from ^{29}Si CP/MAS NMR are displayed in Figure 4. The contact time for cross polarization between ^{29}Si and ^{1}H spins is plotted as abscissa, and the intensity of the signal at −91.5 ppm, as ordinate. The curve is analyzed by the following equation:[24]

$$M(t)=C\left[\exp\left(-\frac{t}{T_{1\rho}H}\right)-\exp\left(-\frac{t}{T_{\mathrm{SiH}}}\right)\right]\left(1-\frac{T_{\mathrm{SiH}}}{T_{1\rho}H}\right)^{-1} \quad (1)$$

Here $M(t)$ is the signal intensity, C is a constant of

(21) Komori, Y.; Enoto, H.; Takenawa, R.; Hayashi, S.; Sugahara, Y.; Kuroda, K. *Langmuir* **2000**, *16*, 5506.

(22) Barron, P. F.; Frost, R. L.; Skjemstad, J. O.; Koppi, A. J. *Nature* **1992**, *302*, 49.

(23) Hayashi, S.; Ueda, T.; Hayamizu, K.; Akiba,E. *J. Phys. Chem.* **1992**, *96*, 10922.

Table 1. Cross Relaxation Times

compds	T_{SiH}/ms
kaolinite	2.2[25]
kaolinite−DMSO-d_6	4.0[25]
kaolinite−DMSO	2.5[25]
kaolinite−*p*NA	0.94

Scheme 1. Schematic Models of (A) Kaolinite, (B) Kaolinite−DMSO-d_6, and (C) Kaolinite−DMSO

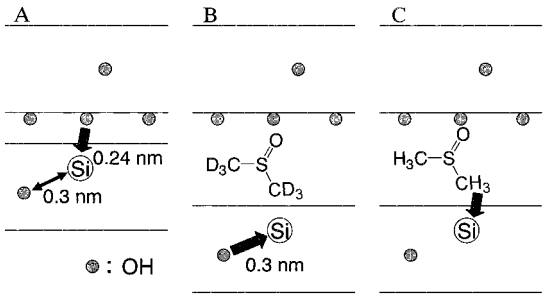

proportionality, $T_{1\rho}H$ is a spin−lattice relaxation time in the rotating frame, and T_{SiH} is a cross relaxation time between ^{29}Si and ^{1}H spins. The results are in good agreement with the eq 1. The fact that the slope of this curve is large indicates that the polarization from ^{1}H to ^{29}Si is fast and that the distance between Si and H is short. The rate of the polarization buildup is expressed by the cross relaxation time between ^{29}Si and ^{1}H spins. The T_{SiH} value for kaolinite/*p*NA was 0.94 ms.

Table 1 lists the reported T_{SiH} values for kaolinite, kaolinite/DMSO-d_6, and kaolinite/DMSO,[25] as well as that of kaolinite/*p*NA synthesized in this study. In the case of kaolinite, the cross polarization takes place from OH groups in the interlayer surface located most closely to Si and T_{SiH} was reported to be 2.2 ms.[25] In the case of kaolinite/DMSO-d_6, the protons nearest to Si are those in the inner-surface hydroxyls and the T_{SiH} value is 4.0 ms.[25] In the case of kaolinite/DMSO, the methyl protons are closest to Si and the T_{SiH} value is 2.5 ms.[25] (Scheme 1). The value of T_{SiH} (0.94 ms) for kaolinite/*p*NA is smaller than those found for the intercalation compounds discussed above. These data indicate that the polarization from ^{1}H to ^{29}Si is fast and that H atoms are present in the neighborhood of Si. On the basis of the XRD data, *p*NA is thought to be arranged in a somewhat inclined manner with respect to the aluminosilicate layers. Consequently, the amino groups should reside on the neighborhood of the silicate sheets.

The IR spectrum of kaolinite/*p*NA is shown in Figure 5. Four bands of OH stretching mode are generally observed for kaolinite at 3620, 3650, 3670, and 3694 cm^{-1}. The band at 3620 cm^{-1} is assigned to inner-surface hydroxyl, which is rarely influenced by intercalation. The other three bands are assignable to outer-surface hydroxyl and perturbed by guest species.[4] The intensity of the band at 3694 cm^{-1} was reduced for the kaolinite/methanol intermediate, and a new band at around 3640 cm^{-1} appeared. After the reaction with *p*NA, the profile was different from those of kaolinite and kaolinite/methanol, suggesting new hydrogen bonds with *p*NA molecules.

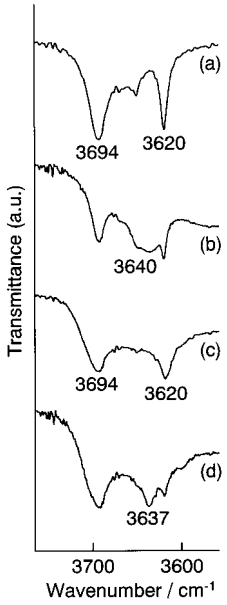

Figure 5. Infrared spectra (OH vibration region) of (a) kaolinite (KBr), (b) kaolinite−methanol intercalation compound (Nujol), (c) kaolinite−*p*NA intercalation compound (KBr), and (d) kaolinite−*o*NA intercalation compound (KBr).

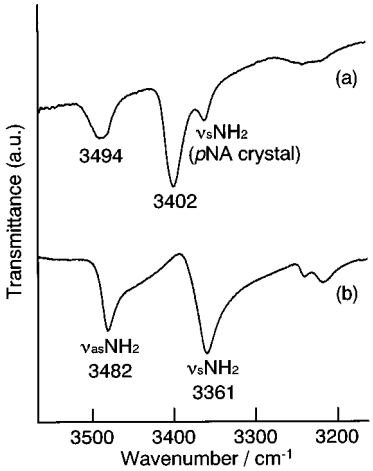

Figure 6. Infrared spectra (NH_2 vibration region: KBr method) of (a) kaolinite−*p*NA intercalation compound and (b) *p*NA crystals.

The bands due to $\nu(NH_2)$ in the kaolinite/*p*NA were observed at 3494 and 3402 cm^{-1} (Figure 6). These bands are shifted to higher wavenumbers than those found in *p*NA crystals (3482 and 3361 cm^{-1}). This result implies that the hydrogen bonds between the amino groups and the silicate sheets are weaker than those in *p*NA crystals. All these results indicate that *p*NA molecules are arranged in one direction. The structural model is depicted in Scheme 2.

Characterization of Kaolinite/*o*NA. The IR spectrum of kaolinite/*o*NA in the OH stretching region is shown in Figure 5. While a broad band was observed at 3640 cm^{-1} for kaolinite/methanol, a relatively sharp band at 3637 cm^{-1} with a small band at around 3600 cm^{-1} were observed for kaolinite/*o*NA. These data support the formation of new hydrogen bondings. The amount of *o*NA in kaolinite/*o*NA was 0.60 *o*NA/[$Al_2Si_2O_5$-$(OH)_4$]. The basal spacing, the IR data, and the *o*NA content suggest that *o*NA molecules take a monolayer arrangement.

(24) Alemany, L. B.; Grant, D. M.; Pugmire, R. J.; Alger, T. D.; Zilm, K. W. *J. Am. Chem. Soc.* **1983**, *102*, 2133.
(25) Hayashi, S.; Akiba, E. *Chem. Phys. Lett.* **1994**, *226*, 495.

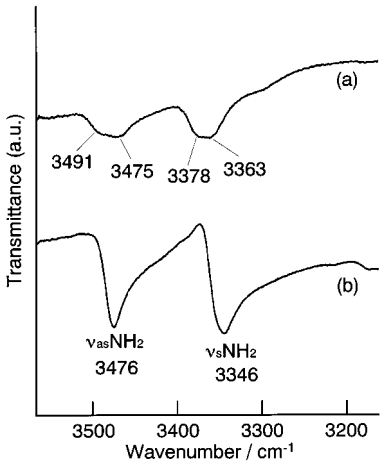

Figure 7. Infrared spectra (NH_2 vibration region: KBr method) of (a) kaolinite−*o*NA intercalation compound and (b) *o*NA crystals.

Scheme 2. Structure Model of the Kaolinite−*p*NA Intercalation Compound

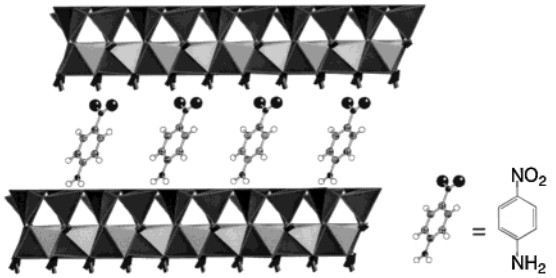

The Si environments of kaolinite/*o*NA were examined by ^{29}Si CP/MAS NMR (Figure 3c). The profile shows a peak at −92.1 ppm with a shoulder at −90.9 ppm. Although the signal at −90.9 ppm may be ascribed to unreacted kaolinite phase, the intense signal at −92.1 ppm strongly supports the intercalation of *o*NA.

The IR spectra of *o*NA and kaolinite/*o*NA in the NH_2 stretching region are shown in Figure 7. The band due to NH_2 symmetric stretching was observed at 3346 cm^{-1} for *o*NA crystals (KBr disk) with asymmetric stretching at 3476 cm^{-1}. After intercalation into kaolinite, *o*NA exhibits the poorly resolved $\nu_s(NH_2)$ bands at around 3378 and 3363 cm^{-1} and broad $\nu_{as}(NH_2)$ bands at around 3491 and 3475 cm^{-1}. These bands are shifted to higher wavenumbers than those for *o*NA crystals. The presence of these bands strongly suggests various kinds of arrangements of *o*NA between the layers.

The ^{13}C CP/MAS NMR spectrum of kaolinite/*o*NA is shown in Figure 2b. The signals (a) due to carbons linked to amino groups were split into multiple peaks, supporting various environments of amino groups. This finding, being consistent with the IR results, implies the diversity of the orientations of *o*NA between the layers.

Second Harmonic Generation. Figure 8 shows UV−vis spectra of kaolinite/*p*NA and kaolinite/*o*NA. For kaolinite/*p*NA, the absorption maximum due to $\pi-\pi^*$ transition was observed at 394 nm. Consequently, there are no absorption bands at around 532 nm; the wavelength is the second harmonic wave of the incident light ($\lambda = 1064$ nm). Kaolinite/*o*NA exhibited the absorption maximum due to the $\pi-\pi^*$ transition at 423 nm. Although the band has some absorption at 523 nm, the SHG intensity was measured similarly as described for the *p*NA case.

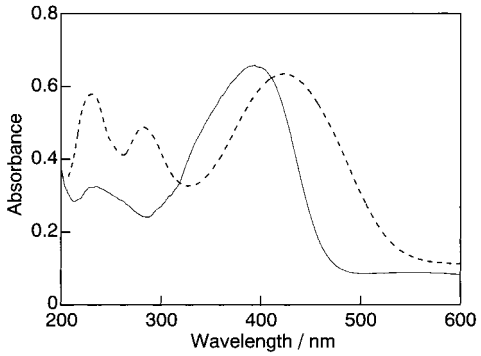

Figure 8. UV−vis spectra of kaolinite−*p*NA intercalation compound (solid line) and kaolinite−*o*NA intercalation compound (dotted line).

Table 2. d_{eff} Coefficients Determined by the SHEW Measurements[a]

sample	d_{eff} rel to urea	d_{eff} absolute/pm V^{-1}
kaolinite	0.05	0.05
kaolinite−*p*NA intercalation compd	7.2	7.9
kaolinite−*o*NA intercalation compd	0.46	0.51
kaolinite−nitrobenzene intercalation compd	0.7	0.77

[a] Both the magnitude relative to urea and the absolute value are presented. The latter is obtained in terms of $d_{11} = 1.1$ pm V^{-1} for the d_{max} of urea.[26]

Table 2 lists the d_{eff} coefficients determined by the SHEW method. Kaolinite/*p*NA was SHG active, and the d_{eff} coefficient was 7.2 times larger than that of urea. The d_{11} component of urea is reported to be 1.1 pm V^{-1}.[26] On the basis of the ratio of the signal intensity of urea to that of kaolinite/*p*NA, the d_{eff} coefficient was estimated to be 7.9 pm V^{-1}. Kaolinite/*o*NA was also SHG active, and the d_{eff} coefficients was estimated to be 0.51 pm V^{-1}. This value is smaller than that of urea.

*p*NA and *o*NA have centrosymmetries in their crystal structures ($P2_1/n$,[27] $P21/a$[28]); thus, SHG is not observed. Although a very low SHG signal is observed for kaolinite itself, the coefficient is 0.05 pm V^{-1} and much smaller than those of kaolinite/*p*NA and kaolinite/*o*NA. Therefore, the SHG observed for the present intercalation compounds mainly arises from interlayer *p*NA and *o*NA. The molecular hyperpolarizability (β) of *o*NA is about 0.3 times that of *p*NA.[20] However, the d_{eff} coefficient of kaolinite/*o*NA is much smaller than that of kaolinite/*p*NA (only 0.06 times). Consequently, *o*NA molecules are not well ordered between the layers, which is consistent with the results of IR and ^{13}C CP/MAS NMR. On the other hand, the hyperpolarizability (β) of nitrobenzene is about 0.09 times that of *p*NA.[20] The d_{eff} coefficient of kaolinite/nitrobenzene was about 0.1 times that of kaolinite/*p*NA. Accordingly, the orientation of guest species in kaolinite/nitrobenzene is as ordered as found in kaolinite/*p*NA and higher than that in kaolinite/*o*NA. This result can be ascribed to the structure where the

(26) Günter, P. *Nonlinear Optical Effects and Materials*; Springer: Berlin, 1999.
(27) Trueblood, K. N.; Goldish, E.; Donohue, J. *Acta Crystallogr.* **1961**, *14*, 1009.
(28) Dhaneshwar, N. N.; Tavale, S. S.; Pant, L. M. *Acta Crystallogr.* **1978**, *B34*, 2507.

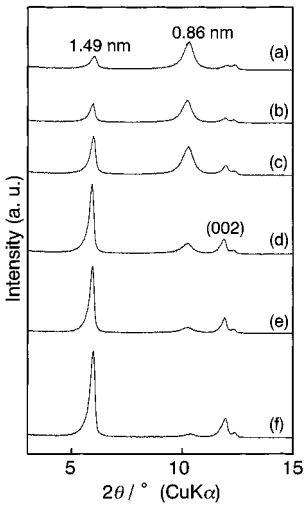

Figure 9. X-ray diffraction patterns of kaolinite−*p*NA intercalation compounds. The reaction time was (a) 3 h, (b) 6 h, (c) 10 h, (d) 15 h, (e) 24 h, and (f) 72 h.

only nitro groups can interact with the interlayer hydroxyl groups, and the interactions result in the high orientation of nitrobenzene.

The amount of *p*NA loaded between the layers was varied by changing the reaction time of formation of kaolinite/*p*NA. The variation of the SHG intensities with the amount was evaluated by a powder method developed by Kurtz.[18] It should be noted that the method is meaningful for qualitative comparison although the method is not so quantitative as the SHEW method. With increase in the reaction time, the intensity of the peak due to the basal spacing (d_{001} = 1.49 nm) of kaolinite/*p*NA increased whereas the intensity of the peak due to dried kaolinite/methanol (d_{001} = 0.86 nm) was decreased. The loaded amount of *p*NA, determined by CHN analysis, increased with the reaction time. Because the XRD peaks due to kaolinite/methanol were observed for the samples with lower loading, *p*NA molecules may be segregated in kaolinite (Figure 9).

Figure 10 shows the relationship of the SHG intensity with the amount of loaded *p*NA. With increase in the amount the SHG intensity increased. Supposing that the effects on both the phase matching and the coherence length are not changed among these materials, the increase in the SHG intensity results from the increase in the amount of *p*NA intercalated. This finding also indicates that the phase intercalated with *p*NA is attributable to the appearance of SHG.

It is now clarified that *o*NA and *p*NA are intercalated into kaolinite whereas *m*NA is not. Selective intercalation of benzenes with two substituents into kaolinite depends on the kind and position of the substituents because of the difference in the interactions between the interlayer surface of kaolinite and the guest species.

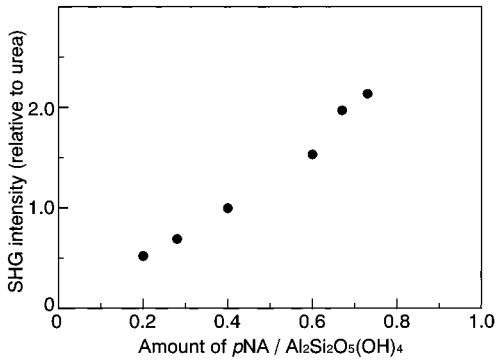

Figure 10. Variation of SHG intensity with the amount of *p*NA.

These phenomena are potentially applicable to selective catalytic effects and stereoselective organic synthesis. Spontaneous orientation of guest species in the unique asymmetrical interlayer region of kaolinite is also useful for organic−inorganic nanomaterials design utilizing photoelectrofunctional molecules.

Conclusions

ortho- and *para*-nitroanilines were intercalated between the layers of kaolinite whereas *meta*-nitroaniline was not. Such a selective intercalation was observed for kaolinite for the first time. In the interlayer region of kaolinite, *para*-nitroaniline adopts a specific orientation where the amino groups are interacting with the oxide sheets of kaolinite and the nitro groups are interacting with the OH groups on the other side. This was supported by the contact time dependencies of the signal intensity of ^{29}Si CP/MAS NMR spectra. *ortho*-Nitroaniline is not oriented in such an ordered way as found in *p*NA, which was indicated by IR and ^{13}C CP/MAS NMR. While SHG is not observed for *ortho*- and *para*-nitroaniline crystals because of their inherent centrosymmetries, kaolinite−*ortho*-nitroaniline and kaolinite−*para*-nitroaniline intercalation compounds exhibited SHG arising from unique and noncentrosymmetric orientations in the interlayers. These spontaneous orientations are induced by the interactions of the guest molecules with the asymmetric interlayer region, which characterize the uniqueness of kaolinite.

Acknowledgment. The authors are grateful to Professor Y. Sugahara (Waseda University) for helpful discussion. This work is supported by a Grant-in-Aid for the Scientific Research by the Ministry of Education, Science, Sports, and Culture of the Japanese Government.

CM010095J